GDCh Communications Angewandte International Edition Chemie

Cluster Compounds

How to cite: *Angew. Chem. Int. Ed.* **2021**, *60*, 645–649
International Edition: doi.org/10.1002/anie.202010342
German Edition: doi.org/10.1002/ange.202010342

Controlled Dimerization and Bonding Scheme of Icosahedral M@Au_{12} (M = Pd, Pt) Superatoms

Emi Ito, Shinjiro Takano, Toshikazu Nakamura, and Tatsuya Tsukuda**

Received: 28 July 2020
Publication Date: 01 October 2020

Swetashree Acharya
27.03.2021

Background

JACS
JOURNAL OF THE AMERICAN CHEMICAL SOCIETY

Article

Cite This: *J. Am. Chem. Soc.* 2019, 141, 15994−16002

pubs.acs.org/JACS

Efficient and Selective Conversion of Phosphine-Protected $(MAu_8)^{2+}$ (M = Pd, Pt) Superatoms to Thiolate-Protected $(MAu_{12})^{6+}$ or Alkynyl-Protected $(MAu_{12})^{4+}$ Superatoms via Hydride Doping

Shinjiro Takano,*[,†] Shun Ito,[†] and Tatsuya Tsukuda*[,†,‡]

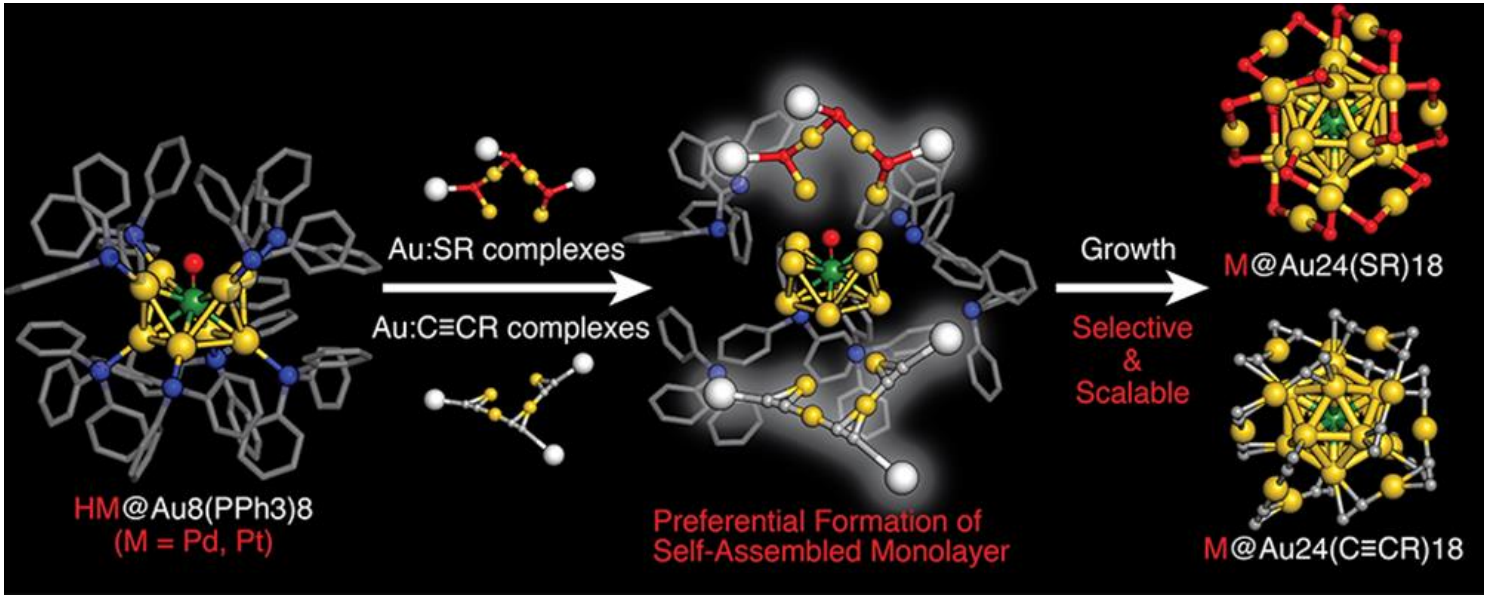

Motivation

- To determine the structure and the spin state of $Pd_2Au_{36}(SR)_{24}$ by more straightforward methods such as SCXRD and static magnetization experiment, respectively.

- To develop an efficient targeted synthesis of superatomic molecules using "preformed" superatoms as starting materials.

Why this paper?

- This paper revealed for the first time, the SCXRD structure of the homo and hetero dimers of M@Au12 superatoms as the cores.

- Hetero-doped MM'$Au_{36}(PET)_{24}$ was synthesized for the first time by using the fusion process of preformed alloy superatoms.

Structure of $Au_{38}(SR)_{24}$

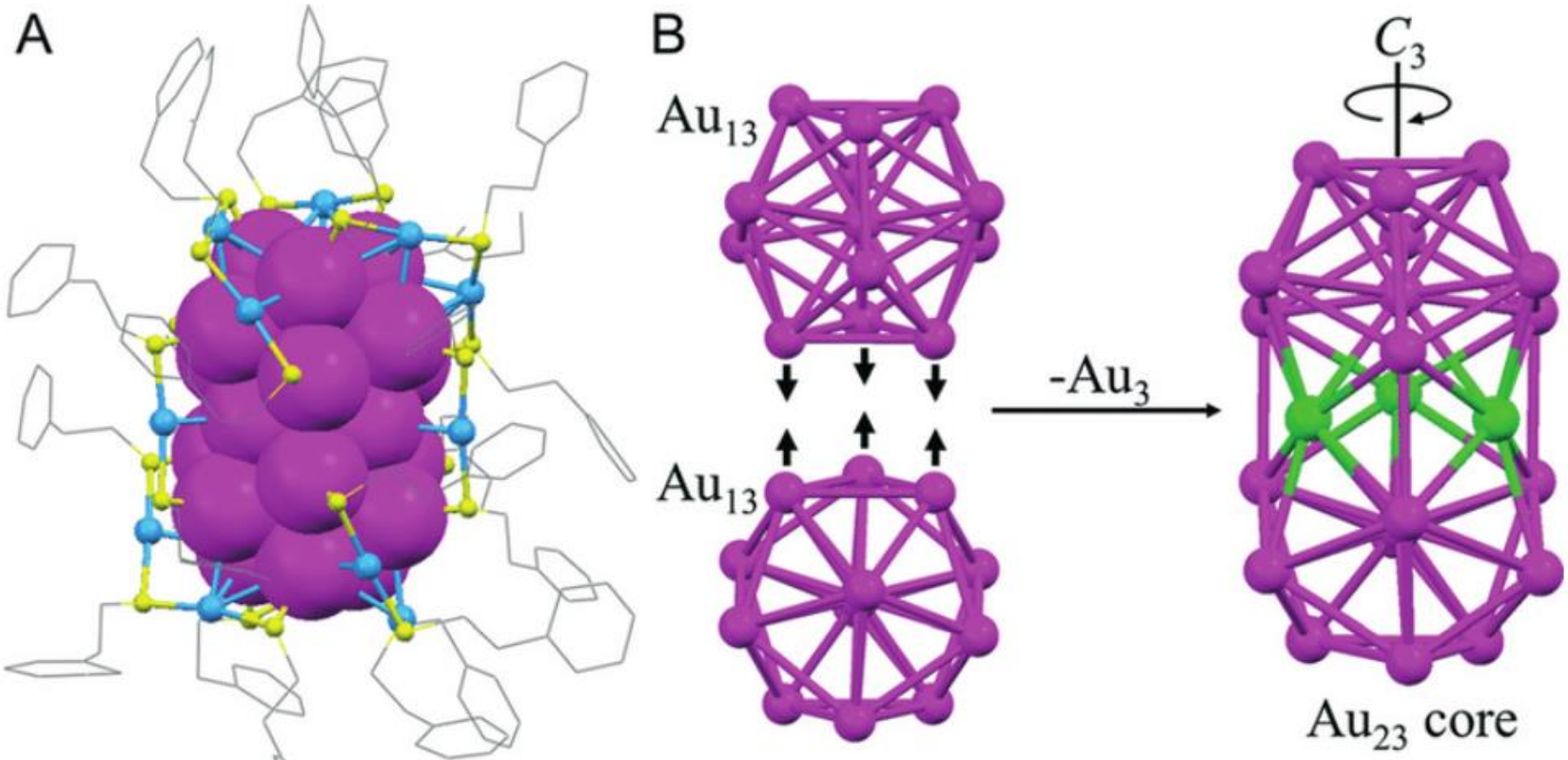

Introduction

- Targeted syntheses of $MM'Au_{36}(PET)_{24}$ (M, M'= Pd, Pt; PET=SC_2H_4Ph) were achieved by hydride-mediated fusion reactions between $[MAu_8(PPh_3)_8]^{2+}$ and $[M'Au_{24}(PET)_{18}]$.

- Single-crystal X-ray diffraction analysis indicated that the products have bi-icosahedral $MM'Au_{21}$ cores composed of $M@Au_{12}$ and $M'@Au_{12}$ superatoms.

- Although the $MM'Au_{21}$ superatomic molecules correspond to O_2 in terms of the number of valence electrons (12 e), the distances between the icosahedrons were larger than that in the bi-icosahedral Au_{23} core of $Au_{38}(PET)_{24}$ corresponding to F_2 and the spin state was singlet.

- These counterintuitive results were explained by a “bent bonding model” based on tilted (non-orthogonal) bonding interaction between the 1P superatomic orbitals of $M@Au_{12}$ and $M'@Au_{12}$ superatoms.

Synthetic procedure

- Firstly, hydrogen-containing clusters $[HPdAu_8(PPh_3)_8]^+$ **(5)** and $[HPtAu_8(PPh_3)_8]^+$ **(6)** were prepared in situ by the reaction of $[PdAu_8(PPh_3)_8]^{2+}$ and $[PtAu_8(PPh_3)_8]^{2+}$ with $NaBH_4$, respectively.

- Then, $PdAu_{24}(PET)_{18}$ and $PtAu_{24}(PET)_{18}$ were reduced to mono-anions $[PdAu_{24}(PET)_{18}]^-$ **(7)** and $[PtAu_{24}(PET)_{18}]^-$ **(8)**, respectively, by mixing with $NaBH_4$.

- Finally, **1**, **2**, and **3** were produced by mixing equivalent amounts of **5** (or **6**) and **7** (or **8**), followed by addition of Au^I-PET oligomer formed in situ by mixing Au^IClSMe_2 and PET-H.

$$5 + 7 + Au^1\text{-PET} = Pd_2Au_{36}(PET)_{24}\ \mathbf{(1)}$$
$$5 + 8 + Au^1\text{-PET} = PdPtAu_{36}(PET)_{24}\ \mathbf{(2)}$$
$$6 + 8 + Au^1\text{-PET} = Pt_2Au_{36}(PET)_{24}\ \mathbf{(3)}$$

Characterization

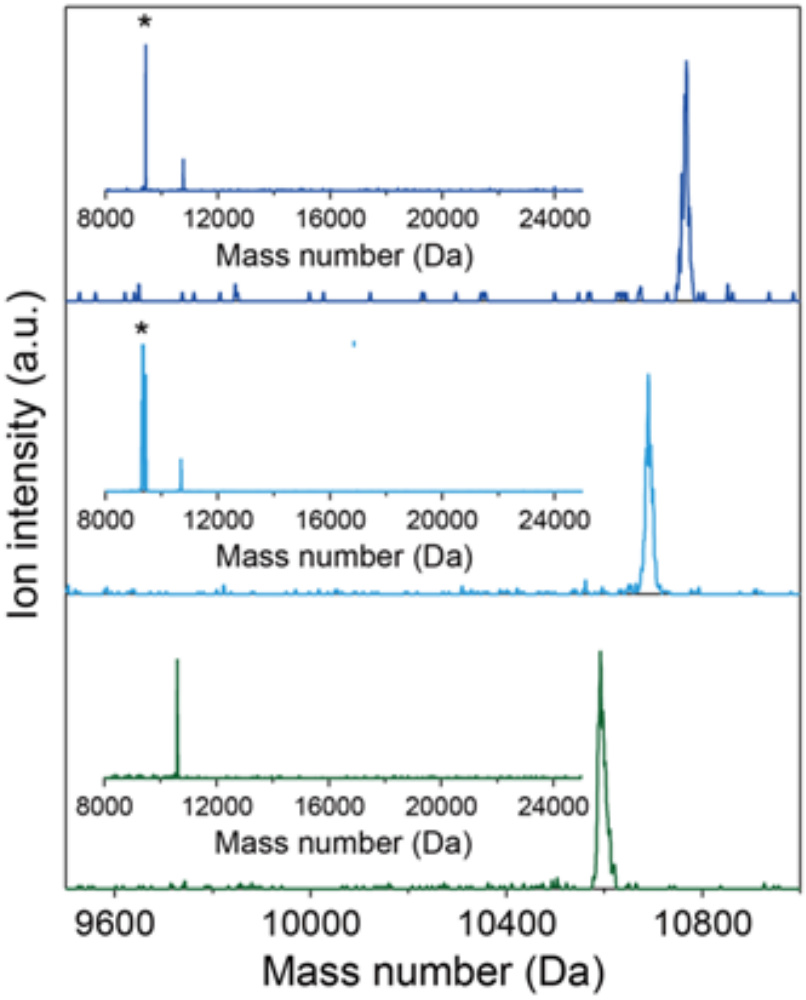

Figure S2. Negative-ion mode MALDI mass spectra of **1** (bottom), **2** (middle), and **3** (top). Inset shows high mass number region. Asterisk indicates the peak corresponding to laser-induced fragmented ion of $(Au\text{-}PET)_4$ loss.

RESULTS AND DISCUSSION

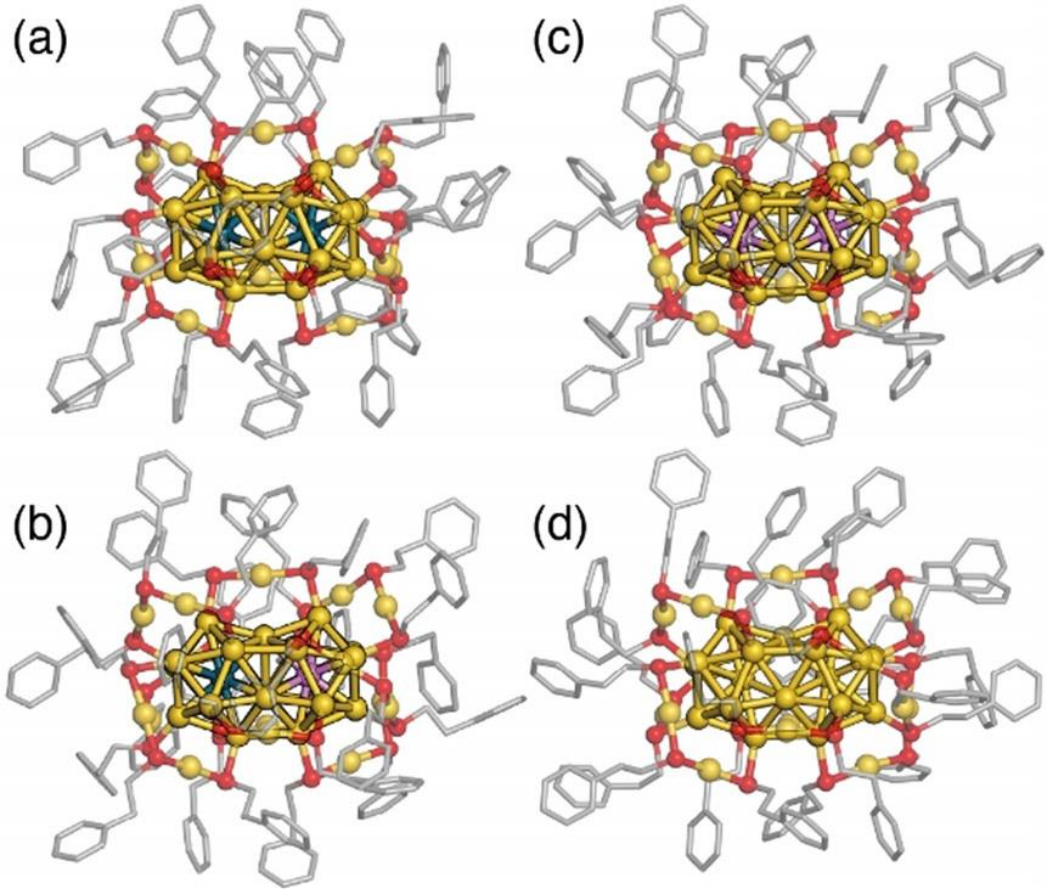

Figure 1. Crystal structures of a) 1, b) 2, c) 3, and d) 4. Metal and sulfur atoms are shown as spheres. Color code: yellow Au; teal Pd; pink Pt, red S, gray C. Organic residues are depicted as gray sticks and H atoms and disordered parts are omitted for clarity. In 2, the central position is treated as half occupancy of Pd/Pt atoms. CCDC numbers are given in the Supporting Information.

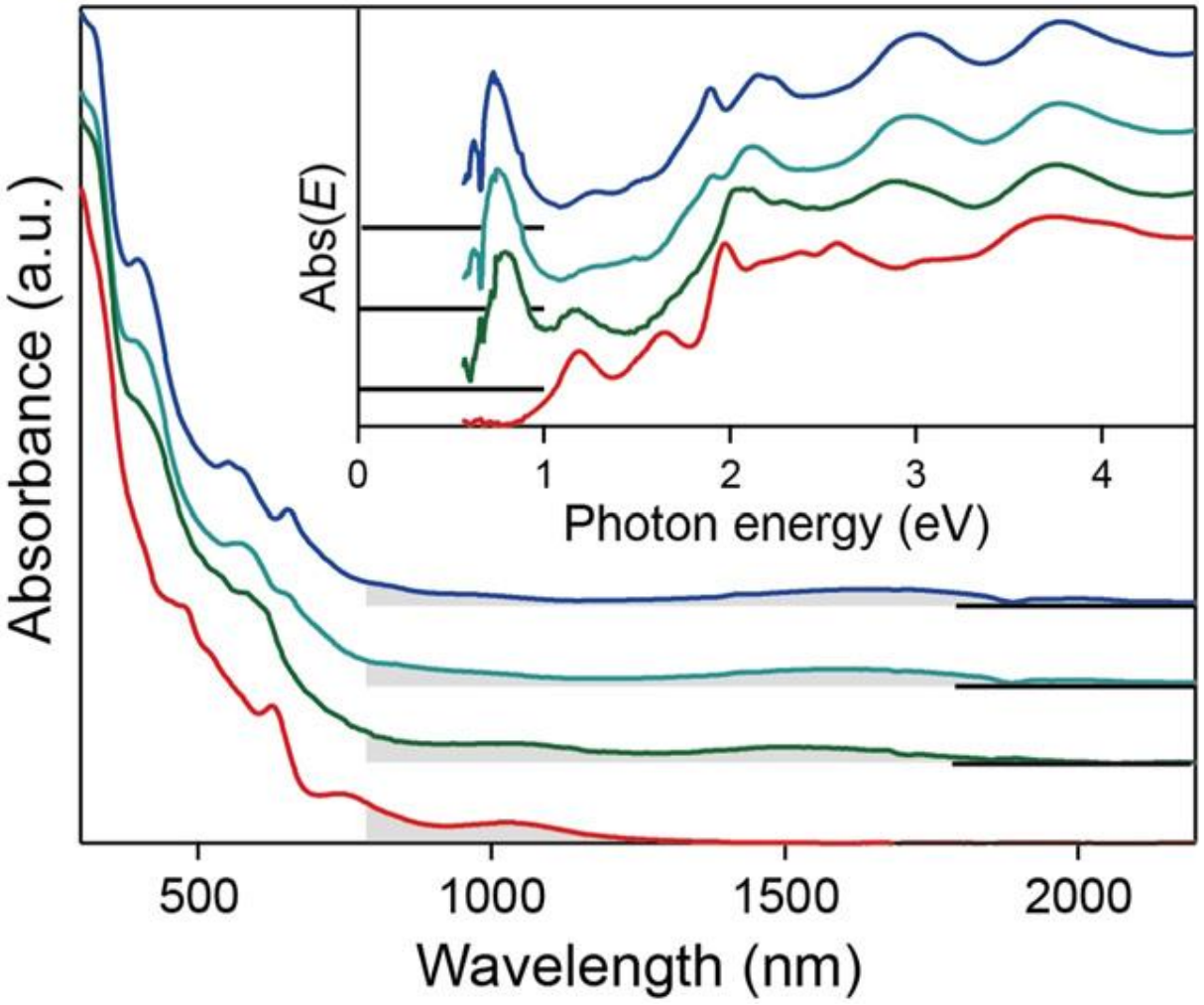

Figure 2. Optical absorption spectra of 1 (green), 2 (cyan), 3 (blue), and 4 (red) in $CHCl_3$. Inset shows the spectra as a function of photon energy obtained by Jacobian transformation. Spectra are offset vertically to avoid the overlapping.

Table 1: Selected structural information of $MM'Au_{21}$ and Au_{23} cores of 1–4.[a]

Cluster	$D_{i\text{-}i}$[b]	$D_{e\text{-}e}$[c]	D_{rb}[d]	D_{sb}[e]	CSM[f]
1[g]	4.133	8.443	2.676–2.840	2.725–3.237	0.298
2[h]	4.136	8.479	2.701–2.824	2.746–3.192	0.238
3[h]	4.151	8.491	2.718–2.828	2.764–3.168	0.228
4[h]	4.087	8.427	2.751–2.835	2.756–3.025	0.305

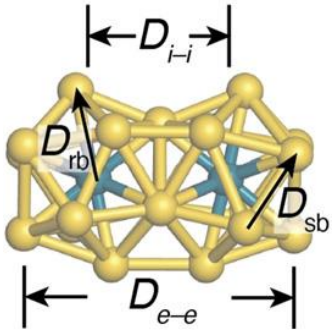

[a] From SCXRD analysis. [b] M-M' distance in . [c] Average distance of both ends in . [d] Radial bond distribution of each icosahedron in . [e] Surface bond (<3.3) distribution of each icosahedron in . [f] Average CSM value of each icosahedron. [g] 103 K. [h] 123 K.

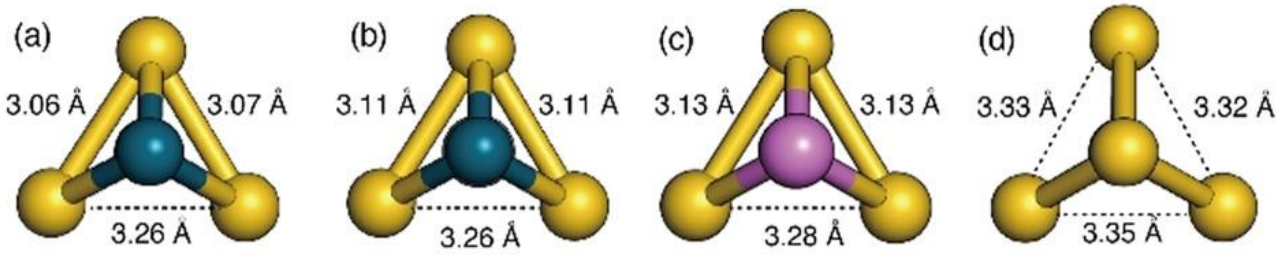

Figure 3. Cross section of the waist of a) Pd_2Au_{21} of 1, b) $PdPtAu_{21}$ of 2, c) Pt_2Au_{21} of 3, and d) Au_{23} of 4.

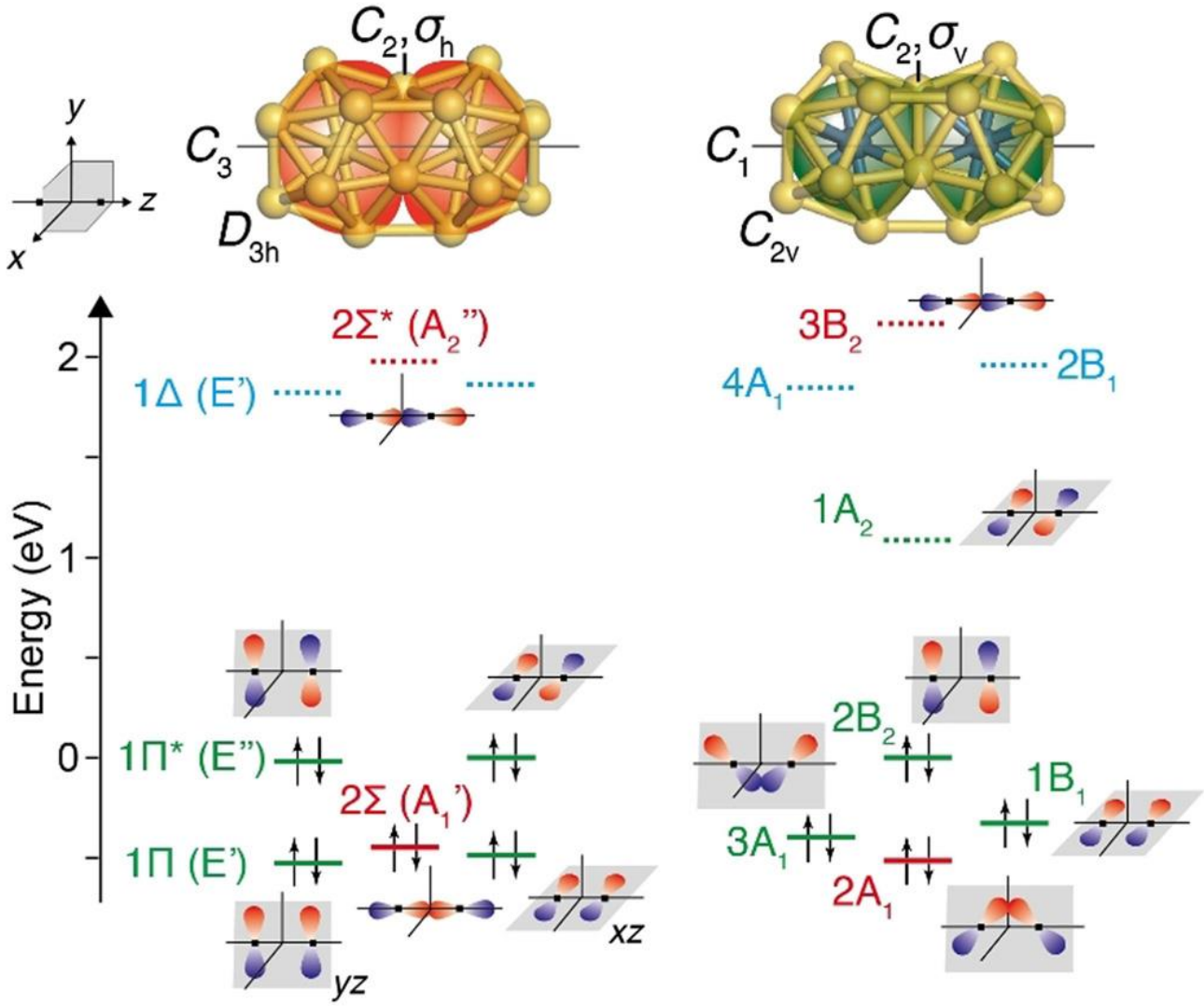

Figure 4. Energy diagrams and schematic Kohn–Sham orbitals of Au_{23} in 4 (left) and Pd_2Au_{21} in 1 (right). Occupied and unoccupied orbitals are represented by solid and dotted lines, respectively.

Conclusion

- Superatomic molecules $MM'Au_{21}$ (M, M'= Pd, Pt) with bi-icosahedral motifs were synthesized by novel fusion reactions between hydrogen-containing $HMAu_8$(8e) superatoms and $M'Au_{12}$(7e) superatoms.

- SCXRD data suggested that the bonds between the icosahedral units in $MM'Au_{21}$ are weaker than that in Au_{23} although the formal bond order of the former is larger than that of the latter.

- Magnetic property measurement revealed that $MM'Au_{21}$ takes a singlet spin state although it can be viewed as O_2 analogue.

- Based on DFT calculation, $MM'Au_{21}$(12e) is constructed through "bent" s and p bonds between the two $Pd@Au_{12}$(6e) superatoms.

THANK YOU